Aalborg Universitet

AALBORG UNIVERSITY
DENMARK

Obtaining the Andersen's chart, triangulation algorithm

Sabaliauskas, Tomas; Ibsen, Lars Bo

Publication date:
2016

Document Version
Publisher's PDF, also known as Version of record

Link to publication from Aalborg University

Citation for published version (APA):
Sabaliauskas, T., & Ibsen, L. B. (2016). *Obtaining the Andersen's chart, triangulation algorithm*. Department of Civil Engineering, Aalborg University. DCE Technical Memorandum No. 53

General rights
Copyright and moral rights for the publications made accessible in the public portal are retained by the authors and/or other copyright owners and it is a condition of accessing publications that users recognise and abide by the legal requirements associated with these rights.

- Users may download and print one copy of any publication from the public portal for the purpose of private study or research.
- You may not further distribute the material or use it for any profit-making activity or commercial gain
- You may freely distribute the URL identifying the publication in the public portal -

Take down policy
If you believe that this document breaches copyright please contact us at vbn@aub.aau.dk providing details, and we will remove access to the work immediately and investigate your claim.

Downloaded from vbn.aau.dk on: May 05, 2023

DEPARTMENT OF CIVIL ENGINEERING
AALBORG UNIVERSITY

Obtaining the Andersen's chart, triangulation algorithm

Tomas Sabaliauskas
Lars Bo Ibsen

ISSN 1901-7278
DCE Technical Memorandum No. 53

Aalborg University
Department of Civil Engineering
Geotechnical engineering

DCE Technical Memorandum No. 53

Obtaining the Andersen's chart, triangulation algorithm

by

Tomas Sabaliauskas
Lars Bo Ibsen

February 2016

© Aalborg University

AAU triaxial Andersen's chart

Tomas Sabaliauskas, Lars Bo Ibsen.

Department of Civil Engineering, Aalborg University

Andersen's chart (Andersen & Berre, 1999) is a graphical method of observing cyclic soil response. It allows observing soil response to various stress amplitudes that can lead to liquefaction, excess plastic deformation or stabilizing soil response.

The process of obtaining the original chart has been improved, and the new method is described in this paper. Algorithm based approximation is introduced, it replaces hand made lines with computer generated curves. This makes the obtained estimates more reliable and once implemented the procedure is faster than the original method.

1. INTRODUCTION

The original work done by (Andersen & Berre, 1999) on undrained cohesionless soil response is the starting point of this paper. In their original work they approximated cyclic response of soil during stress cycles on triaxial samples and summarized the results in an Andersen's chart (Fig.7). Similar project was undertaken by (Troya & Sabaliauskas, 2014) using an improved triaxial apparatus in Aalborg University. The latter authors used a computer algorithm to generate the Andersen's chart from the data they collected (Fig.12).

Soil used

The chart starts from measuring real soil response. Samples of Frederikhaven sand were dry tamped to 80% relative density (maximum porosity e_{max}=1.05; minimum porosity e_{min}=0.64);

All samples were tested from initial conditions of pore pressure ΔUp = 200[kPa], initial confining pressure p'_0=60[kPa]. Anisotropic K0 consolidation is applied to reassemble in situ soil state for cohesionless soil with friction angle of approximately φ=39° giving initial sample state of σ_1=161[kPa] σ_3=60[kPa];

The saturated sample (of saturation beyond 99% saturation judging by Skempton's B) is exposed to cycles of constant stress amplitude. Different stress amplitude $\boldsymbol{\tau_{cy}}$ and average stress values $\boldsymbol{\tau_a}$ for every test (parameters ilustrated in Fig.1). The two parameters are chosen in such a way to provoke 10% strain in approximately 1000 cycles or less. They cluster around liquefaction sensitive areas in the Andersen's chart (the boundary between stable and liquefying soil as shown in Fig.6)

Axial strain is logarithmically corrected to represent true strain rather than engineering strain. This is necessary because strain beyond 10% can be encountered, engineering strain becomes increasingly less precise as large strain is applied.

During triaxial testing effective stress states are monitored, thus all plots in this paper and the Andersen's chart it self are by default in effective stress state. Compression is taken as positive loading direction with respect to geotechnical sign convention.

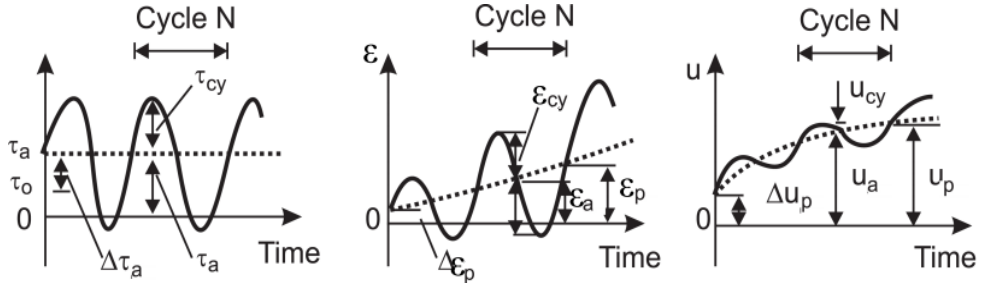

Eq. 1

Fig. 1 cyclic, average and plastic components of shear stress, strain and pore pressure (Andersen & Berre, 1999)

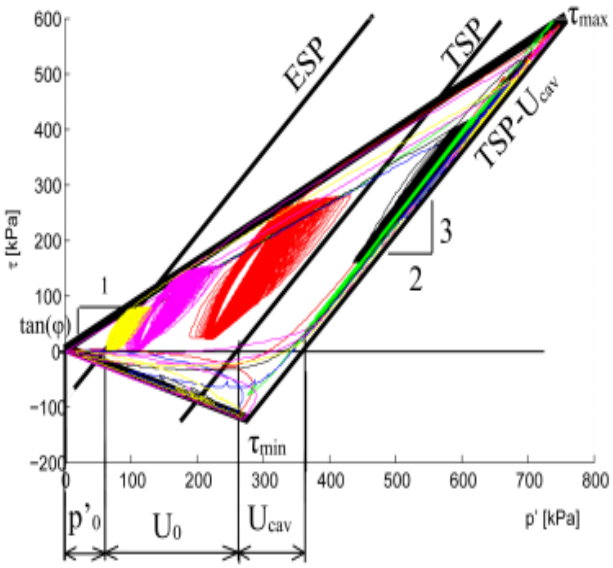

Fig. 2 Multiple cyclic tests followed by ultimate bearing capacity crushing. Contained in a "triangle" consisting of friction angles and cavitation limit.

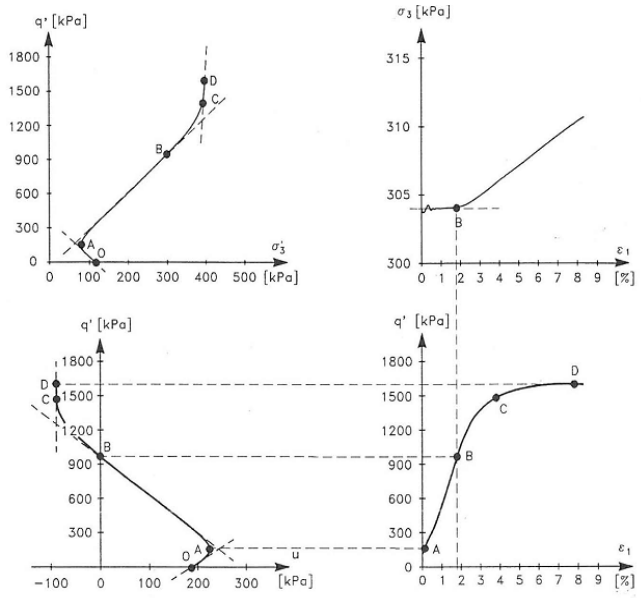

Fig. 3 pore pressure and strain of Monotonic CU triaxial on Baskarp no 15. (Ibsen, 1995)

2. UNDRAINED BEARING CAPACITY

To draw the boundaries of undrained Andersen's chart it is important to recognize where the physical limits of the chart are. There is a limited ammount of load that can be applied on a soil sample, thus all the loading scenarios going beyond this limit need to be avoided. By drawing the boundary of undrained bearing capacity one can quickly observe the testing limits within which the tests will be executed.

If the sample was loaded drained it would follow the Effective Stress Path (ESP line in Fig. 2). Undrained dense soil fails at much higher load than drained ones due to dilation induced pore pressure drop. Pore pressure can drop all the way to cavitation, where water transforming into a gas. Once the dilating sample "pulls the water apart" the liquid water becomes into gas and there is nothing to further resist soil deformation. Thus the point of cavitation limits undrained dilative soil strength. The undrained limit can be seen in Fig. 2, by the name of Total Stress Path minus the negative cavitation pressure (TSP-Ucav),

When dense sand is compressed to failure undrained it dilates at close proximity to friction angle (points A-B-C in Fig. 3). At some point pore pressure will reach near -100[kPa] and turn into gas (Point C-D). As the stiffness of water is lost pure plastic response will follow (from point D in Fig. 3, TSP-Ucav in Fig. 2).

Cavitation plays a very definitive role in response of undrained, dense, cohesionless soil. The transitions into cavitation a strict limit on ultimate strength (Fig. 2, Fig. 4). This was not taken into account in original work of Andersen (Fig. 5), probably because he used very high pore pressure during his tests. This should have pushed the undrained bearing capacity beyond the testing range of his equipment. Non the less, the undrained limit imposed by cavitation is shown to play a decisive role in multiple other studies. (Ibsen, 1994) (Ibsen, 1995)(Nielsen & Ibsen, 2013) (Troya & Sabaliauskas, 2014). The maximum and minimum undrained bearing capacity can be found from equations (2-3).

The undrained and drained boundary can be observe in Fig.4, where drained test is compared to 3 different kind of undrained tests, all with similar density.

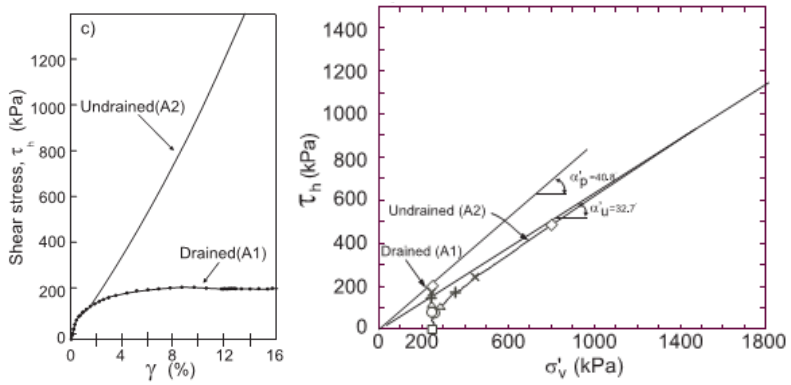

Fig. 5 Andersen's stress-strain chart and principal stress DSS test – undrained response does not reach plastic failure due to extremely high initial pore pressure available for dilation. (Andersen & Berre, 1999)

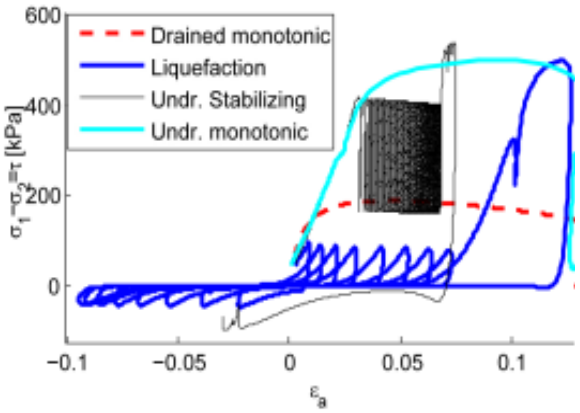

Fig. 4 cavitation limit in multiple loading cases. Strain given in raw measurements, for % expression multiply by 100.

$$p'_{LOCK} = p'_0 + U_0 - Ucav \qquad (1)$$

$$\tau_{max} = -p'_{LOCK} \cdot \sin(\varphi)/(\sin(\varphi) - 1) \qquad (2)$$

$$\tau_{min} = -p'_{LOCK} \cdot \sin(\varphi)/(\sin(\varphi) + 1) \qquad (3)$$

The provided bearing capacity expressions include effects of pore pressure and quantify the absolute limit of soil strength. Thus it is proposed to normalize undrained soil response using these strength limits. (Nielsen & Ibsen, 2013)

3. BOUNDARIES IN STRESS SPACE

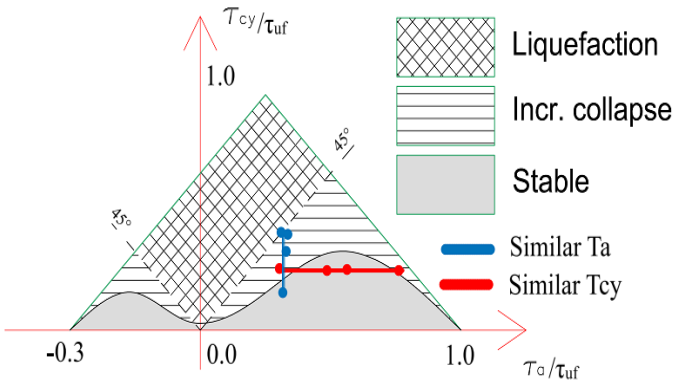

Fig. 6 Normalized schematic of observed response

Each sample starts from anisotropic – K0 state which is loaded over 1 hour of slow, drained loading. Then the valves are closed and a cyclic, sinusoidal shaped load is applied.

The sinusoidal load shape is good for one sided loading – a loading case where absolute value of τ_a is bigger than τ_{cy}.

Testing indicated that stress reversal ($|\tau_a| < \tau_{cy}$) cause liquefaction even at very small stress amplitudes, by increasing ever increasing strain amplitudes. Incremental collapse was confirmed to occur if stress is not maintained sufficiently high wihtihn one sided loading (Fig. 6). (Sabaliauskas & Troya, 2014).

During cyclic loading failure was defined as 10% axial strain. If 10% strain amplitude did not accumulate after 1000th cycles the sample was deemed stable. 1000 cycle limit was chosen because it approximates the number of waves during a 3 hour storm peak in typical storm in North Sea. The ε=10% is equivalent to shear strain limit of γ=15% used by Andersen & Berre, 1999.

During testing it was observed that 1000 cycles produce a very steep function separating stable response from unstable. In Fig. 6 position of test with similar τ_a and τ_{cy} are shown. Small difference in stress can have significant impact on soil response, and testing is very slow, thus it is important to target the zones of interest within the chart.

Strain stabilizes with cycles, producing increasingly more horizontal curve. It is necessary to interpolate along this flat curve for reliable approximation of the number of cycles that lead to 10% strain (shown in Fig.9). This is hard to do by hand (Fig.7), but a computer algorithm will easily detect the first cycle to cross the 10% boundary.

By using the undrained ultimate shear strength τ_{max} to normalize the chart one can scale the bearing capacity for different soil states as long as the TSP+Ucav (Fig.2) is scaled properly. Thus the limits between 1 and 0 are in respect to undrained strength for triangle shown in Fig. 6.

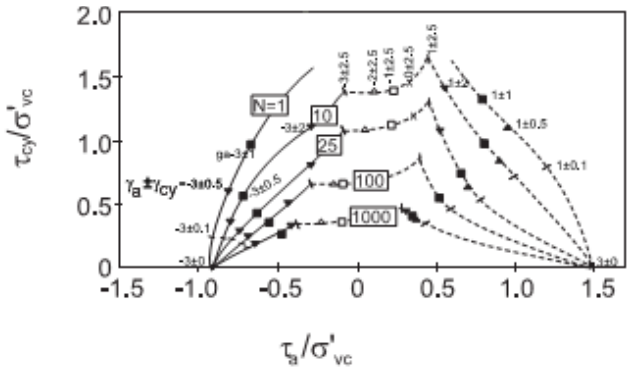

Fig. 7 Original Andersen's chart for undrained soil response (normalized by drained confining pressure)

4. DATA PROCESSING FOR ANDERSEN'S CHART

Obtaining coordinates of data points

Three points need to be found for each data point in the chart - τ_a, τ_{cy} and the number of cycles **n** leading to a selected strain limit. These are obtained by detecting stress peaks inside measurements (Fig.9).

Averaging high peak and low peak stress values of the true applied shear average was also necessary (Fig. 10). The samples were loaded with a force, but as the samples deform the area of cross section changes and the effective stress generated by the same applied force is somewhat fluctuating.

Number of cycles when ε limit is reached are found by identifying the first data point to cross above the 10% stain limit. When that data point is known algorithm checks how many stress peaks are present before that point in testing history (Fig. 9). The 3 values, 2 for stress and 1 for cycles, are saved for each test.

Adding some pre defined data points helps to fill in the gaps without executing new tests. For instance all points with amplitude τ_{cy}=0[kPa] are stable. If applied amplitude is zero, the sample will not fail unless τ_a reaches the ultimate undrained failure limit. 1000 cycles of zero amplitude is nothing more than keeping a stable load applied, thus it is safe to say that **n**=1000 at points of τ_{cy}=0[kPa] where $\tau_a < \tau_{max}$.

If $(\tau_a+\tau_{cy})>\tau_{max}$ or $(\tau_a-\tau_{cy})<\tau_{min}$ then sample will cross the ultimate shear strength before completing the first cycle. Thus the outer perimeter of the triangle in is set to **n**=0 cycles. The points are distributed along the boundary to form convenient grid for future interpolation.

Interpolating

At this point the chart will be interpolated by triangulation. A surface is formed by connecting the nearest points into a triangular surfaces (Delaunay triangulation). As more tests are done definition of the chart will continuously increase Fig. 11. However some fine tuning by hand can increase the diagram precision as well.

Increasing chart definition manually

If charts in Fig.11 and Fig.12 Are compared it is easy to see that one of them has "smooth" edges while the other has some glitches.

The original way to increase precision of the chart is to monitor for glitches observed in algorithm generated plot at early development stages. This allws to target the next test position. The plot can be updated indefinitely. Yet in some times manual adjustment of the Delaunay triangulation could be much faster than setting up a new test.

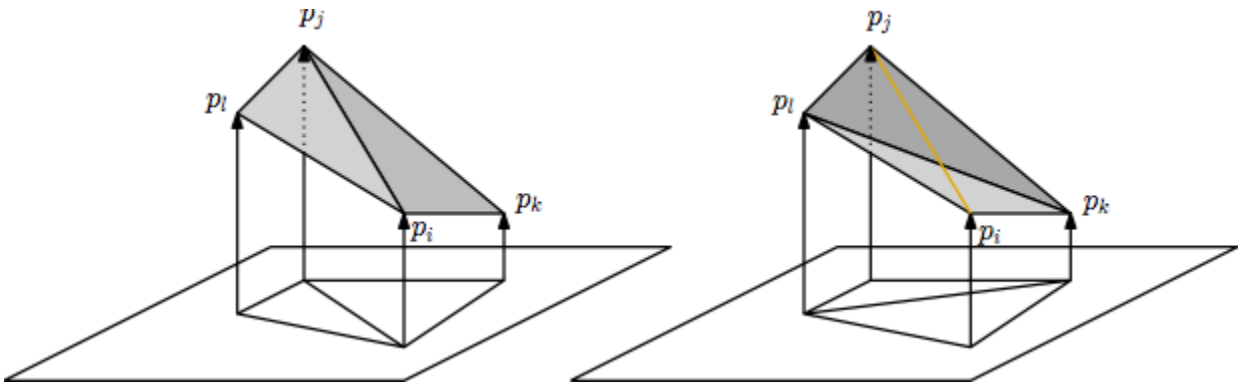

Fig. 8 "Edge flipping". There are 2 ways of connecting the same 4 points. Manual identification of the correct one might be necessary.

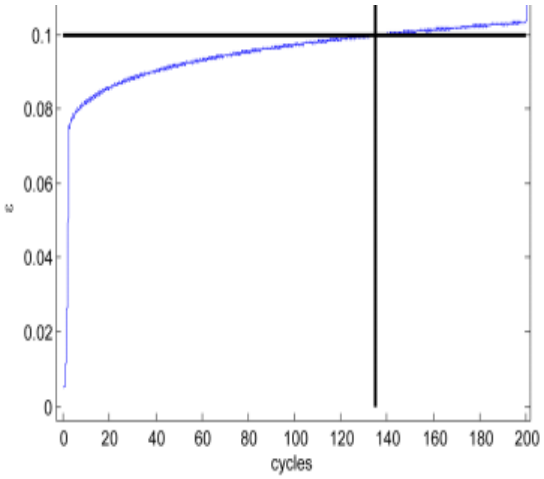

Fig. 9 Strain development with cycles and Strain peak detection.

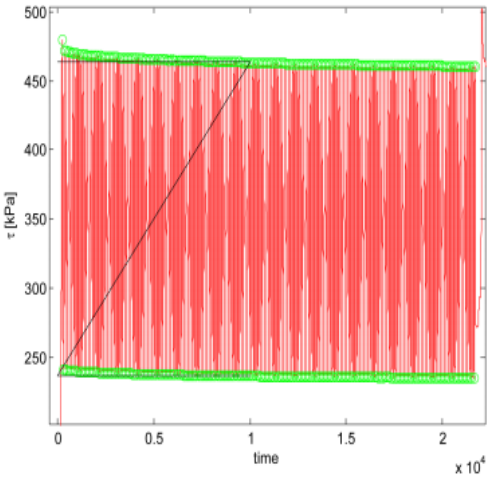

Fig. 10 stress peak identification and position of averaged values

One option previously mentioned is interpolating similar lines which means adding a point of 1000 cycles where the user is certain the soil is stable, or adding an n=0 point at the physical limits.

The other option comes directly from arbitrariness induced by Delaunay triangulation itself (Fig. 8). There are 2 ways of connecting 4 points that are not on the same plane. It can either be connected as a "mountain" (Fig. 8, left) or as a "valley" (Fig. 8, right). As the number of sample points increases this difference will converge towards zero, but looking at a course chart in Fig. 11 it is obvious where the "valleys" are. An averaged cycle count, in the middle between pj and pi can be inserted by hand in Fig. 8, by interpolating one point manually. It is up to user to decide where new points can be added, but it common sense to avoid extrapolating outside from in-between two real data points.

In the liquefying zone (Fig.6) it was found that much smaller stress amplitudes cause liquefaction than those triangulation linearly interpolated, while values of higher stress do not stabilize even in pure compression cycles – thus some **n**=0 points were added in the liquefying area to reduce the triangulation error. This was a case of cautious extrapolation based on observed soil response. The final surface of loading cycles leading to 10% strain is shown in Fig.12.

Once the algorithm is implemented, the 10% limit can be varied and undrained Andersen's chart of varying sensitivity will be produced. However, because the transition from liquefaction to stable state is so steep and fragile, additional tests will likely be necessary, as the position of transitioning lines could shift.

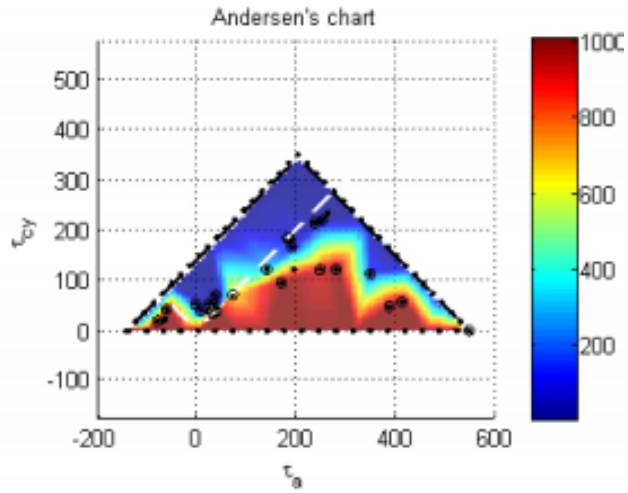

Fig. 11 Andersen's chart before manual corrections. Dots indicate tested points. Fully autonomous generated by algorithm – some triangulation error present.

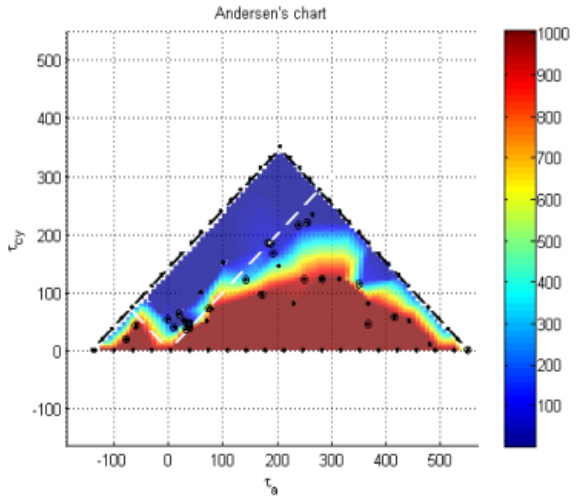

Fig. 12 Andersen's chart for Frederic haven silty sand – not normalized, raw data for 10% axial strain limit.

5. BIBLIOGRAPHY

Andersen, K. & Berre, . T., 1999. *Behaviour of a dense sand under monotonic and cyclic loading comportemen,* Amsterdam: European Conference on Soil Mechanics and Geotechnical Engineering.

Andersen, K. H., 2009. *Bearing capacity under cyclic loading — offshore,.* Oslo: The 21st Bjerrum.

Hettler, A. & Vardoulakis, I., 1984. *Behaviour of dry sand tested in a large triaxial apparatus.* s.l.:Geotechnique 34.2 (1984): 183-197..

Ibsen, L. B., 1994. *The stable state in cyclic triaxial testing on sand.* Aalborg: Soil Dynamics and Earthquake Engineering 13 (1994) 63-72 .

Ibsen, L. B., 1995. *The Static and Dynamic Strength of Sand.* Copenhagen: European Conference on Soil Mechanics and Foundation Engineering.

Nielsen, S. D. & Ibsen, L. B., 2013. s.l.:International Society of Offshore and Polar Engineers.

Praastrup, U., Jakobsen, K. P. & Ibsen, L. B., 1999. *Two Theoretically Consistent Methods for Analysing Triaxial Tests.* Aalborg: Computers and Geotechnics. Vol. 25(1999), pp. 157-170.

Sabaliauskas, T. & Troya, A., 2014. *Observations during static and cyclic undrained loading of dense Aalborg University sand no. 1.* Aalborg: DCE Technical Memorandum No. 43.

Shajarati, A., Sørensen, K. W., Dam, S. K. & Ibsen, L. B., 2012. *Manual for Cyclic Triaxial Test.* Aalborg: DCE Technical Report No. 114.

Troya, A. & Sabaliauskas, T., 2014. *Cyclic behaviour of undrained dense Aalborg University sand no. 1.* Aalborg: DCE Technical Memorandum. Department of Civil Engineering, Aalborg University,.